Letters

A Segmented Rogowski Coils Based Noninvasive Monitoring Method of Current Imbalance in Press Pack IGBTs

Yuanfang Lu, Xiangyu Zhang, *Member, IEEE*, Hong Shen, Wuyu Zhang, and Lei Qi

***Abstract*—Press pack insulated-gate bipolar transistor (PP IGBT) plays an essential role in high-capacity power electronic transmission equipment. Due to the influence of various factors, such as structural pressure and temperature in practical operation, the internal parallel chips of the IGBT may experience inevitable current imbalance, which cannot be detected by existing method. This letter proposes a segmented Rogowski coil (SRC) based noninvasive monitoring method of current imbalance in PP IGBT. By segmenting the standard Rogowski coils around the IGBT device and measuring them individually, the general distribution of the current inside the device can be perceived. After detailed analysis of the mutual inductance characteristics and transfer function, a prototype of SRC was developed. The theoretical model of SRC has been verified by measuring a single current-carrying wire, with an error of only 1.21%. The effectiveness of the proposed scheme was demonstrated by using it to monitor the current distribution in different directions for the same IGBT device.**

***Index Terms*—Imbalanced current, noninvasive monitoring, press pack insulated-gate bipolar transistor (PP IGBT), segmented Rogowski coil (SRC).**

I. Introduction

PRESS pack insulated-gate bipolar transistor (PP IGBT) has been widely used in high-voltage direct current transmissions, large-capacity power converters, and new energy power generation since their advantages of high-power density, double-sided heat dissipation, and easy series connection [1], [2], [3].

To increase the current capability further, PP IGBT usually requires paralleling multiple chips. However, as shown in Fig. 1, the imbalanced current between multiple chips is inevitable since the imbalance of pressure, the parameter variation of chips, the impact of stray inductance in packaging, etc., which will result in degradation of devices' performance [4], [5]. Therefore, the condition monitoring of imbalanced current is significant for the safe operation of devices and equipment.

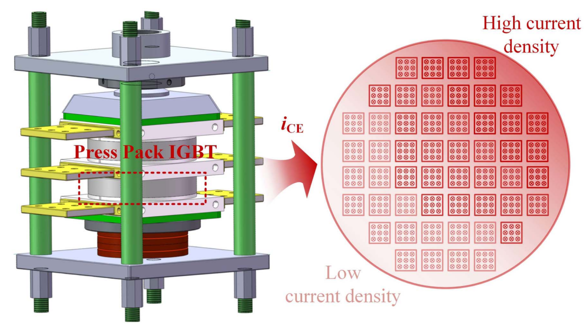

Fig. 1. Imbalance of the parallel chips' currents inside IGBT.

To detect the current distribution of PP IGBT, some Rogowski coils (RCs) based works have been done [5], [6], [7], [8]. A type of miniature RC was developed by Furuya and Ishiyama [8], which was used to measure the current distribution of three chips in PP IGBT. Further, Bock et al. [7] obtained the current distribution of a PP IGBT with eight chips densely arranged during turn-ON process using RCs winding by hand.

Compared with the above traditional RCs, printed-circuit board (PCB) RC has advantages of small size and easy integration [9], which is very suitable to be embedded in PP devices. Jiao et al. [6] proposed a PCB RC mounted on the pedestal of PP IGBT to measure the currents of four chips inside the device. Additionally, to minimize influence of electric and magnetic field interference, Fu et al. [5] introduced promising design methods of turns arrangement, lead wires, and shielding layers, which reduce the measurement error to 1.8%.

However, although monitoring the current of each individual chip is highly precise, it requires a proportional number of sampling circuits, which can be prohibitively expensive and superfluous. In the engineering context, precise knowledge of individual chip currents is not necessary. Rather, it is sufficient to obtain the approximate state of current imbalance in device as a guide for replacement purposes. Additionally, the invasive methods mentioned above require opening the package of the device and installing sensors inside, which may increase the size of the device and compromise its hermeticity and insulation, ultimately reducing its reliability.

Manuscript received 19 May 2023; revised 13 June 2023; accepted 22 June 2023. Date of publication 4 July 2023; date of current version 1 September 2023. This work was supported in part by the National Natural Science Fund for Distinguished Young Scholars under Grant 52225701, and in part by the Fundamental Research Funds for the Central Universities under Grant 2023YQ003. *(Corresponding author: Xiangyu Zhang.)*

The authors are with the State Key Laboratory of Alternate Electrical Power System With Renewable Energy Sources, North China Electric Power University, Beijing 102206, China (e-mail: luyuanfang@ncepu.edu.cn; zhangxiangyu@ncepu.edu.com; shenhong1995@outlook.com; 120202101022@ncepu.edu.cn; qilei@ncepu.edu.cn).

Color versions of one or more figures in this article are available at https://doi.org/10.1109/TPEL.2023.3292263.

Digital Object Identifier 10.1109/TPEL.2023.3292263

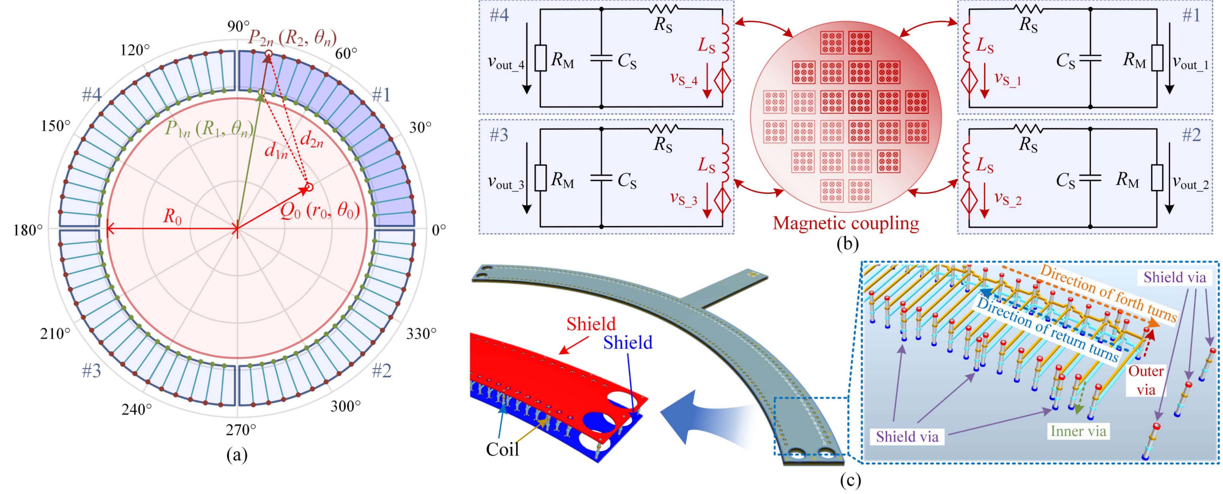

Fig. 2. (a) Schematic of the proposed nonintrusive detection method. (b) Equivalent circuit model of the proposed method. (c) Structure of the proposed SRC.

TABLE I
COMPARISONS WITH EXISTING METHODS

Method	Integration method	Number of sampling circuits	Accuracy of measurement
Typical RC [7], [8]	Invasive	Equal to the number of chips	High
PCB RC [5], [6]	Invasive	Equal to the number of chips	High
This work	Noninvasive	Four	Low

To address the above issue, a segmented Rogowski coils (SRCs) based noninvasive monitoring method of current imbalance is proposed in this letter. A standard circular PCB RC is segmented into several symmetrical segmented RCs and arranged around the device. Due to SRCs' unique mutual inductance characteristics, measurements can provide valuable guidance on the approximate current distribution of PP IGBT, without compromising its structural integrity. As shown in Table I, while the proposed method may have lower accuracy than existing invasive methods, its noninvasiveness and fewer required sampling circuits offer significant advantages, making it more suitable for engineering applications.

The rest of this letter is organized as follows. In Section II, the design concept of SRCs is introduced, and their mutual inductance characteristics and the relationship between their output voltage and the current distribution of the device are analyzed. A single current-carrying wire measurement experiment and two double-pulse testing experiments were done to verify the theoretical analysis in Section III. Finally, Section IV concludes this letter.

II. NONINVASIVE DETECTION METHOD OF CURRENT IMBALANCED IN PP IGBTS

A. Segmented Design of Rogowski Coils for Current Imbalance Monitoring

The standard circular RC possesses rotational symmetry due to its symmetric circular structure, which renders the mutual inductance of the region it surrounds essentially constant. When the RC is segmented, its rotational symmetry is disrupted, resulting in nonuniform mutual inductance with surrounding area. However, this change may bring certain advantages in certain applications, such as current imbalance monitoring for PP IGBT. The proposed noninvasive monitoring method and its structure are shown in Fig. 2(a) and (c), SRCs' measurements can provide guidance on the approximate current distribution of devices since their special mutual inductance characteristics.

As the number of segments increases, the perception of current distribution becomes more precise. However, this comes at the cost of decreased sensitivity due to the reduction in mutual inductance of the SRCs. Taking into account the above considerations, this letter introduces the proposed method using a typical design of four SRCs. The SRC used in this article is implemented using a four-layer PCB as shown in Fig. 2(c). Each SRC has 88 turns, and an integrated differential coil structure was adopted to counteract any possible vertical magnetic flux [9]. The top and bottom layers serve as shielding, while the coil is arranged in the middle.

B. Mutual Inductance Characteristics of SRCs

For any SRC, the mutual inductance M_0 between it and any point Q_0 in the area of device can be expressed as [10]

$$M_0\left(r_0,\theta_0\right)=\frac{\mu_0 \mathrm{a}}{2\pi}\sum_{n=1}^{N}\left[\ln d_{2n}\left(r_0,\theta_0\right)-\ln d_{1n}\left(r_0,\theta_0\right)\right] \quad (1)$$

where a is the height of each rectangular turn, and μ_0 is the permeability of air, which equals $4\pi\times10^{-7}$ H/m. r_0, θ_0, d_{1n}, d_{2n}, and N are the distance and angle of Q_0 from the pole, the distances from Q_0 to the inner edge and outer edge of the nth rectangular turn, and the total number of turns of the SRC, respectively. $d_1(n)$ and $d_2(n)$ can be obtained as (2). To simplify the analysis, the polar coordinate system is adopted in this letter

$$\begin{cases} d_{1n}\left(r_0,\theta_0\right)=\sqrt{R_1^2+r_0^2-2R_1 r_0\cos\left(\theta_n-\theta_0\right)} \\ d_{2n}\left(r_0,\theta_0\right)=\sqrt{R_2^2+r_0^2-2R_2 r_0\cos\left(\theta_n-\theta_0\right)} \end{cases} \quad (2)$$

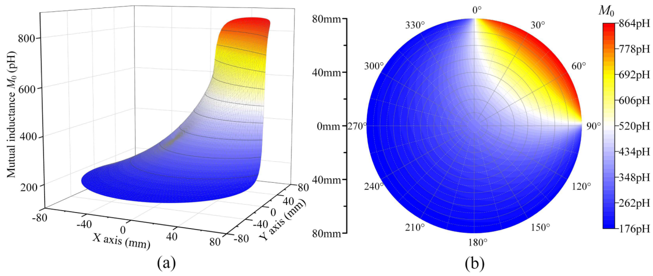

Fig. 3. (a) 3-D diagram of mutual inductance of SRC. (b) Polar contour map of mutual inductance of SRC.

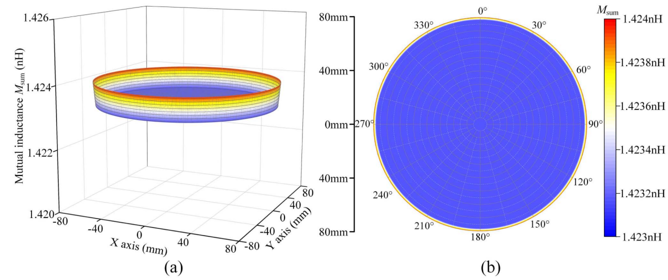

Fig. 4. Sum of the mutual inductances of the four SRCs. (a) 3-D diagram. (b) Polar contour map.

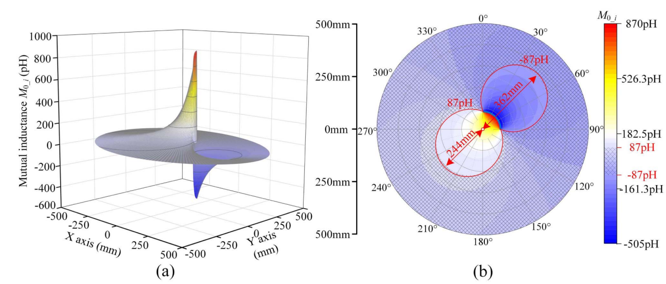

Fig. 5. (a) 3-D diagram of mutual inductance of SRC. (b) Polar contour map of mutual inductance of SRC.

where R_1 and R_2 are the inner and outer radius of the SRC, respectively. θ_n is the angle of the *n*th rectangular turn in the polar coordinate system.

Taking the SRC #1 in Fig. 2(a) as an example, its mutual inductance is depicted in Fig. 3 using (1) and (2) with $N = 88$, $a = 0.33$ mm, $R_1 = 81$ mm, $R_2 = 86$ mm, and the radius of device $R_0 = 80$ mm. As shown in Fig. 3, the SRC is more sensitive to the current in adjacent areas, and its mutual inductance decays dramatically with increasing distance, which provides the possibility for the detection of imbalanced current in the device.

C. Equivalent Model and Transfer Function

The equivalent circuit model of the system is shown in Fig. 2(b). The four SRCs have the same self-inductance L_S, parasitic resistance R_S, parasitic capacitance C_S, and sample resistor R_M. $v_{S\cdot i}$ and $v_{\text{out}\cdot i}$ ($i = 1,\ldots,4$) are the induced voltage and the corresponding output voltage, respectively.

For the current through unit area dS of the device, its corresponding induced voltage can be described as

$$dv_{S\_i} = M_{0\_i}\frac{\mathrm{d}J}{\mathrm{d}t}\mathrm{d}S \tag{3}$$

where J is the current density and $M_{0\cdot i}$ is the mutual inductance between the dS and the SRC #*i*.

For the current through unit area dS, the transfer function of its corresponding output voltage is given by

$$\frac{\mathrm{d}v_{out\_i}(s)}{J(s)\mathrm{d}S} = \frac{sM_{0\_i}}{s^2L_SC_S + s\left(\frac{L_S}{R_M} + R_SC_S\right) + \frac{R_S}{R_M} + 1}. \tag{4}$$

As shown in (4), the current through the unit area is differential with its corresponding output voltage during the frequency is much lower than the self-resonant frequency of the SRC, which has the same characteristics of standard RCs.

The output voltages of the SRCs can be obtained as follows by integrating (4):

$$v_{out\_i}(s) = \iint_S \frac{sM_{0\_i}J\left(s\right)}{s^2L_SC_S + s\left(\frac{L_S}{R_M} + R_SC_S\right) + \frac{R_S}{R_M} + 1}\mathrm{d}S. \tag{5}$$

For any coils, $J(r_0, \theta_0)$ are same and $M_{0\cdot i}(r_0, \theta_0)$ are symmetric about the pole. So the output voltages of the SRCs can provide useful guidance for the imbalanced current of the device since their mutual inductance characteristics are mentioned above. Furthermore, the sum of the four SRCs' output voltages is shown in (6), where M_{sum} is the sum of the mutual inductances of the four SRCs, which approximates a constant, as shown in Fig. 4. Obviously, the sum of the output voltages of the four SRCs is equivalent to the output voltage of a complete circular RC, which can provide a standard value as a reference for the device's current

$$\begin{cases} v_{\text{sum}}(s) = \sum\limits_{i=1}^{4} v_{\text{out\_1}}(s) = \iint_S \frac{sM_{\text{sum}}J(s)}{L_SC_Ss^2 + R_SC_Ss + 1}\mathrm{d}S \\ M_{\text{sum}} = M_{0\_1} + M_{0\_2} + M_{0\_3} + M_{0\_4}. \end{cases} \tag{6}$$

D. Discussion on Interference of External Sources

Typical RCs only couple to the current passing through their interior and does not couple to external sources since their closed structure. However, this characteristic is destroyed on the SRC due to its segmented design. Therefore, it is necessary to discuss the interference caused by external sources.

The mutual inductance of the SRC with the current within a radius of 500 mm around the center of the device is shown in Fig. 5. As we can see, the impact of external sources on SRC decreases as the distance increases. To maximize the measurement reliability of SRCs, it is imperative to ensure that the SRCs and the device under test are located as far as possible from external sources. This may limit the online monitoring application of the proposed method in some compact structures. In these scenarios, the proposed method is better suited as an offline means of maintenance and operation detection.

III. Experimental Verification

To verify the mutual inductance characteristics of SRCs, two SRCs were placed at different positions around a current-carrying wire with a maximum current of 120 A and operating

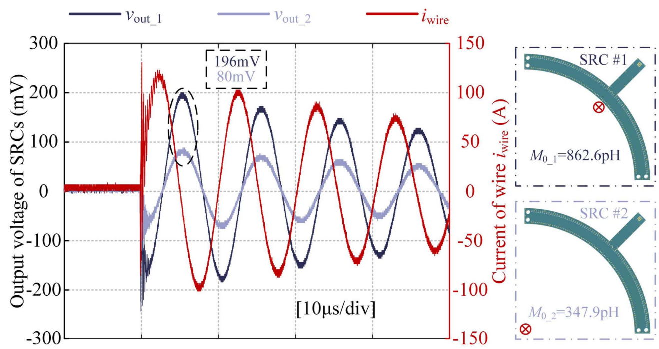

Fig. 6. Measurement results of the current-carrying wire.

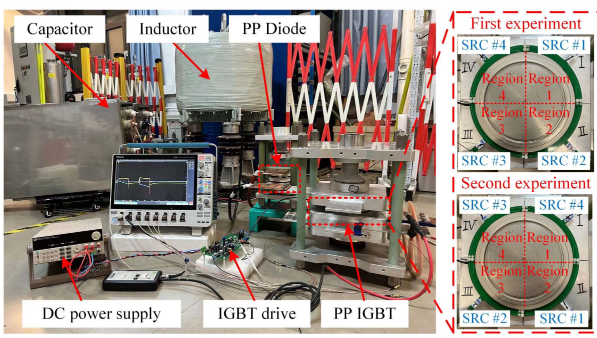

Fig. 7. Double-pulse test bench and placement of SRCs.

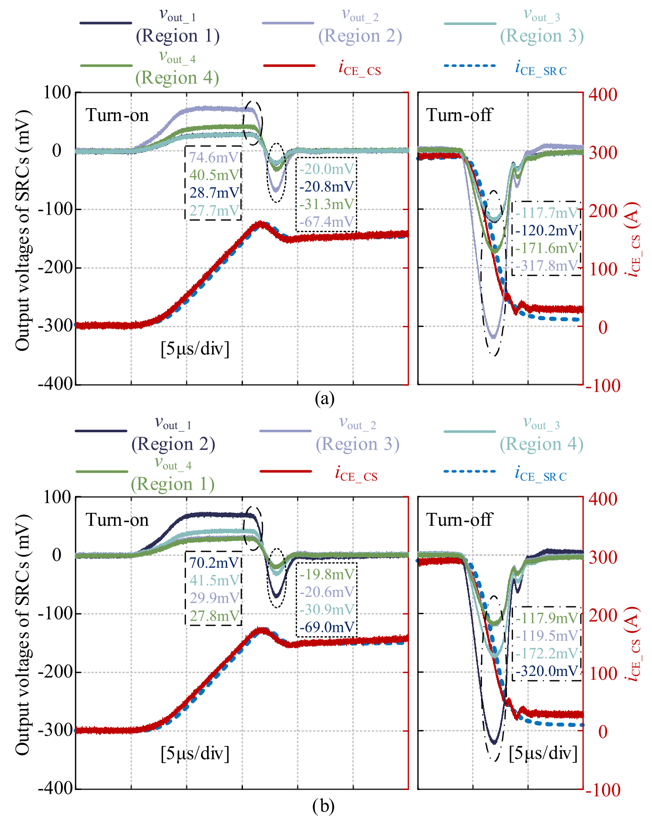

Fig. 8. (a) First experiment's waveforms of the $i_{\mathrm{CE\cdot CS}}$, $i_{\mathrm{CE\cdot SRC}}$, and the output voltages of SRCs. (b) Second experiment's waveforms of the $i_{\mathrm{CE\cdot CS}}$, $i_{\mathrm{CE\cdot SRC}}$, and the output voltages of SRCs.

at 100 kHz. A mixed signal oscilloscope MSO58 is employed to capture the waveforms. As shown in Fig. 6, the amplitude ratio of the output voltages of two RSCs is 2.45, and they are proportional to the derivative of the wire's current. The calculated mutual inductances between each of the two SRCs and the wire are 862.6 and 347.9 pH, respectively, with a ratio of 2.48 between them. The ratio of output voltages differs from the theoretical model by only 1.21%, indicating that the mutual inductance model is highly accurate.

A double-pulse test bench was prepared, as shown in Fig. 7. The capacitance value is 16 mF, the inductance value is 0.2 mH, and the charging voltage of the capacitor is 200 V. The type of PP IGBT used in the test bench is T2960BB45E from IXYS. A current sensor is used to measure the actual current of the PP IGBT $i_{\mathrm{CE\cdot CS}}$.

Since the limitations of experimental conditions and device ageing, the current of PP IGBT is hard to achieve complete balance. Therefore, to illustrate the effectiveness of the proposed method, two control experiments were done, and the SRCs were rotated 90° around the center in two experiments, as shown in Fig. 7.

The waveforms of the first experiment and the second experiment are shown in Fig. 8(a) and (b), respectively. As observed, the output voltages of all SRCs exhibited a linear relationship with the $\mathrm{d}i_{\mathrm{CE\cdot CS}}/\mathrm{d}t$. Based on (6), the sum of the output voltages of the four SRCs was subjected to numerical integration, resulting in a calculated current $i_{\mathrm{CE\cdot SRC}}$ that matches the measured actual current $i_{\mathrm{CE\cdot CS}}$ well. According to the analysis in Section II, the ratio of output voltages of SRCs can serve as an indicator to evaluate the current distribution of the PP IGBT. As we can see, although the SRCs were placed differently in the two experiments, the ratio of output voltages of SRCs in the two experiments are approximately equal, which proved the effectiveness of the proposed method. Since the SRCs' special mutual inductance characteristics, we can conclude that the PP IGBT's current is imbalanced, with more current in Region 2 and less current in Region 1 and Region 3. The output voltages of SRCs show slight differences between the two experiments, which can be attributed to experimental errors caused by minor misalignments of SRCs.

IV. Conclusion

In this letter, a novel noninvasive monitoring method of current imbalanced in PP IGBTs is proposed. The standard RC was segmented and placed around the PP IGBT, the general current distribution inside the device can be obtained based on their measurement results. Finally, a single current-carrying wire measurement experiment and two double-pulse testing experiments were completed to verify the effectiveness of the proposed method. Compared with existing methods, the proposed method does not require compromising devices' structural integrity or additional sensors inside the devices, which is more conveniently and safely applied in engineering. Additionally, it should be noted that the proposed method is incapable of detecting axisymmetric current imbalances, which will be address in our future article.

References

[1] F. Filsecker, R. Alvarez, and S. Bernet, “Comparison of 4.5-kV press-pack IGBTs and IGCTs for medium-voltage converters,” *IEEE Trans. Ind. Electron.*, vol. 60, no. 2, pp. 440–449, Feb. 2013.

[2] Z. Chen, J. M. Guerrero, and F. Blaabjerg, “A review of the State of the art of power electronics for wind turbines,” *IEEE Trans. Power Electron.*, vol. 24, no. 8, pp. 1859–1875, Aug. 2009.

[3] A. Q. Huang, “Power semiconductor devices for smart grid and renewable energy systems,” *Proc. IEEE*, vol. 105, no. 11, pp. 2019–2047, Nov. 2017.

[4] C. Peng, X. Li, J. Fan, Z. Zhao, X. Tang, and X. Cui, “Experimental investigations on current sharing characteristics of parallel chips inside press-pack IGBT devices,” *IEEE Trans. Power Electron.*, vol. 37, no. 9, pp. 10672–10680, Sep. 2022.

[5] S. Fu et al., “Current measurement method of multiple chips using rectangular PCB Rogowski coils integrated in press pack IGBT device,” *IEEE Trans. Power Electron.*, vol. 38, no. 1, pp. 96–100, Jan. 2023.

[6] C. Jiao, Z. Zhang, Z. Zhao, and X. Zhang, “Integrated Rogowski coil sensor for press-pack insulated gate bipolar transistor chips,” *Sensors*, vol. 20, no. 15, 2020, Art. no. 4080.

[7] B. Bock, E. U. Krafft, and A. Steimel, “Measurement of multiple chip currents in a press-pack IGBT using Rogowski-coils,” in *Proc. Eur. Power Electron. Conf.*, 2003, pp. 1–10.

[8] M. Furuya and Y. Ishiyama, “Current measurement inside press pack IGBTs,” *Fuji Elect. J.*, vol. 75, no. 8, pp. 1–3, 2002.

[9] Y. Shi, Z. Xin, P. C. Loh, and F. Blaabjerg, “A review of traditional helical to recent miniaturized printed circuit board Rogowski coils for power-electronic applications,” *IEEE Trans. Power Electron.*, vol. 35, no. 11, pp. 12207–12222, Nov. 2020.

[10] S. Fu, X. Li, Z. Zhao, and X. Cui, “A concise analytical formula of mutual inductance for circular Rogowski coil revealing spatial distribution characteristics of mutual inductance deviation,” *IEEE Sens. J.*, vol. 22, no. 16, pp. 16055–16066, Aug. 2022.